WARSAW UNIVERSITY OF TECHNOLOGY Index 351733
FACULTY OF CIVIL ENGINEERING
COMMITTEE FOR CIVIL AND WATER ENGINEERING
POLISH ACADEMY OF SCIENCES ISSN 1230-2945

DOI: 10.24425/ace.2024.149885

ARCHIVES OF CIVIL ENGINEERING

Vol. LXX ISSUE 2 2024

pp. 629 –642

Research paper

Design and optimization analysis of pylon open lower corbel

Dong Li[1]

Abstract: This study, centered around the engineering context of the Wuxue Yangtze River Bridge, addresses the challenge of significant temperature-induced secondary internal forces in the short lower tower column. A novel open lower corbel tower scheme is proposed as a solution. Firstly, comprehensive finite element models are established for both the open lower corbel pylon scheme and the traditional lower continuous beam pylon scheme. These models are employed for finite element analysis to derive bending moments and displacements of the bridge pylon under various loads, including permanent, vehicle, temperature, and wind loads. Subsequently, considering internal force distribution and stiffness, a comparative assessment is made between the open lower corbel cable pylon scheme and the traditional lower continuous beam cable pylon scheme. The findings reveal that the open corbel structure bridge pylon exhibits lower transverse bending moment values under the influence of permanent load, vehicle load, temperature load, and wind load. This reduction is advantageous for mitigating the issue of significant temperature-induced secondary internal forces in the bridge pylon. Additionally, the transverse bridge stiffness of the open lower corbel cable pylon scheme is found to be on par with that of the lower continuous beam cable pylon scheme. Moreover, topology optimization of the original corbel design is accomplished using the relative density method. The computational results demonstrate that the corbel's stress and deformation under vertical loads meet code requirements. These research findings offer valuable insights for the design and construction of similar projects.

Keywords: internal force, lower corbel, optimization, pylon, stiffness

[1]MSc., The 1st Engineering Company Limited, China Railway Construction Bridge Engineering Bureau Group, 116033, Dalian, China, e-mail: 67183150@qq.com, ORCID: 0009-0009-3881-4521

1. Introduction

Long-span cable-stayed bridges usually adopt floating system and semi-floating system [1–3]. It is a common practice to set vertical support under the main beam at the bridge tower for semi-floating system cable-stayed bridges. Usually, the lower beam is set in the bridge tower and the support is placed on the lower beam to provide the vertical support for the main beam. However, there may be a situation where the lower tower column is relatively short due to terrain restrictions, resulting in a large temperature internal force of the bridge tower. By changing the construction process of the lower cross beam, the secondary internal force generated in the construction process can be reduced, such as Jingyue Yangtze River Bridge and Jiayu Yangtze River Bridge [4]. Although this scheme reduces the problem of temperature secondary internal force in construction engineering, the problem of large temperature internal force after completion of the bridge has not been solved [5, 6].

In addition to setting the support to provide vertical support for the main beam, zero cable can also be set [7]. The zero cable cancels the lower beam and suspends the cable from the center of the bridge tower to provide vertical support for the main beam [8]. Qingshan Yangtze River Bridge has adopted the zero cable scheme. The zero cable solves the problem of large temperature secondary internal force of the lower tower column, but there is no longitudinal stiffness support of the lower beam, which reduces the seismic resistance of the whole bridge structure [9].

In this paper, open lower corbel is proposed to solve the problem of obvious secondary internal force caused by the short lower tower column of Wuxue Yangtze River Bridge. The lower corbel and place the support on the corbel to provide vertical support for the main beam. Compared with the traditional beam scheme and zero cable scheme, this scheme fully considers the internal force and stiffness of the bridge tower, which can solve the problem of large temperature secondary internal force of the lower tower column, and provide sufficient longitudinal stiffness for the main beam. In this paper, the corbel scheme and the traditional beam scheme are compared and analyzed from the perspective of the internal force and deformation of the bridge tower structure. At the same time, the topology optimization of the corbel scheme is carried out to further improve the structural performance.

2. Project profile

Wuxue Yangtze River Highway Bridge is an asymmetric cable-stayed bridge with a main span of 808 meters. It adopts a semi-floating structural system. The bridge span is arranged as (80 meters + 290 meters + 808 meters + 75 meters + 75 meters + 75 meters). The height of the north main tower is 269 meters, and the lower beam is set up between the towers. The height of the south main tower is 233.602 meters, and the height of the lower tower is only 21.602 meters, as shown in Fig. 1.

If the same lower beam structure as the north tower is adopted, due to the shorter lower tower column of the south main tower, a large secondary internal force will be generated under the action of temperature, shrinkage and creep and a large number of transverse

(a)

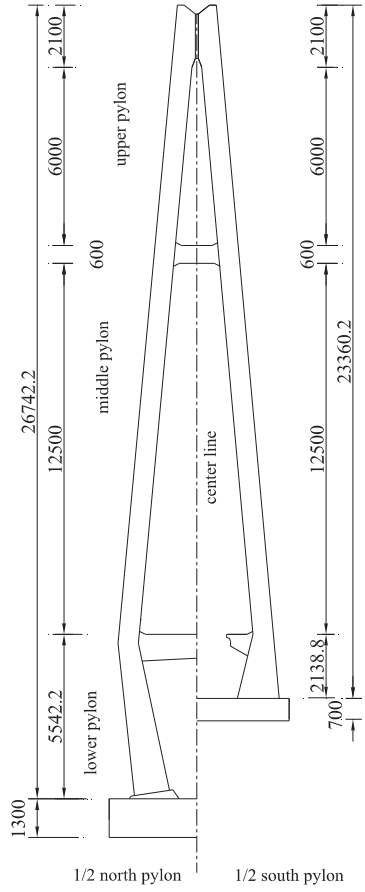

(b)

Fig. 1. Layout diagram of Wuxue Yangtze River bridge:
a) elevation, b) elevation of the bridge tower (cm)

prestress. It is easy to cause concrete cracking of the bridge tower. At the same time, the use of a lower lower beam structure will also reduce the overall aesthetic effect of the bridge tower. The south main tower adopts the open lower corbel instead of the traditional beam structure to solve this problem. The open lower corbel scheme can effectively reduce the secondary internal force of the lower tower column of the south tower under the action of temperature, shrinkage and creep and transverse prestress, so as to avoid the occurrence of concrete cracking. The overall aesthetic effect of the bridge tower of this scheme is improved.

3. Analysis of mechanical properties of bridge tower

The full-bridge spatial finite element models of the two schemes are established, which are the traditional beam scheme and the corbel scheme. The cross section and cable force of the two schemes are consistent. The concrete main girder, steel box girder, pylon and cross beam are simulated by beam element, the stay cable is simulated by cable element, the support is simulated by elastic connection, and the bottom of the pylon is treated as consolidation in the model.

The computed loads encompass various permanent effects, such as structural weight, shrinkage, creep, and prestress. Additionally, the analysis incorporates the overall temperature variations experienced by the entire tower, encompassing temperature changes in the tower structure, the impact of vehicle loads, and the influence of wind loads. The temperature fluctuations considered involve a rise of 20°C and a reduction of 30°C. The vehicle load adheres to China Highway Load-I standards, and the wind load acting on the tower is quantified at 28.2 kN/m. The loading combination is determined by a specific formula: 1.4 times the vehicle load plus 1.05 times the temperature action minus 0.825 times the wind load. This comprehensive approach ensures a thorough consideration of multiple factors contributing to the structural loading conditions.

3.1. Internal force analysis

3.1.1. Transverse utility of bridge tower under permanent action

From top to bottom, the extreme bending moment sections of the tower are the top and bottom of the upper tower column, the top and bottom of the middle tower column, and the top and bottom of the lower tower column. The transverse bending moment diagram of the bridge tower under permanent load is shown in Fig. 2. The main difference in the bending moment of the bridge tower is reflected in the lower tower column. The transverse bending moment at the bottom of the lower tower column of the lower beam pylon scheme is 1181918.5 kN·m, while the transverse bending moment at the bottom of the lower tower column of the open lower corbel pylon scheme is 710295.9 kN·m, the difference between the two is 471622.6 kN·m. It is worth noting that the bending moment of the open lower corbel tower scheme is larger at the top of the lower tower column. This is because the corbel belongs to the cantilever structure, under the action of the reaction force of the support, the bending moment at the top of the lower tower column increases.

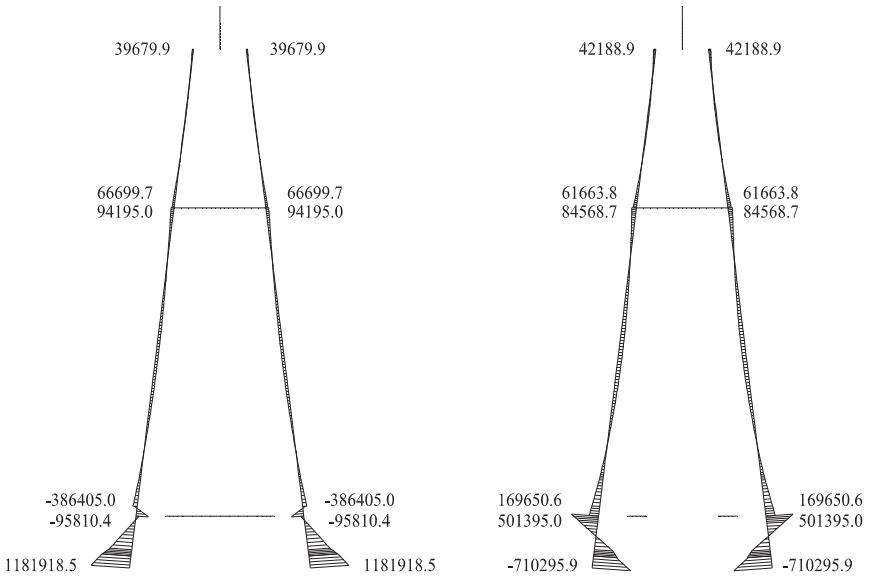

Fig. 2. Transverse bending moment of bridge tower under permanent action (kN·m): a) beam scheme, b) corbel scheme

Define the ratio coefficient.

$$\alpha = \frac{M_b - M_c}{M_c} \times 100\% \tag{3.1}$$

where: M_b represents the bending moment of the beam scheme and M_c represents the bending moment of the corbel scheme.

When $\alpha > 0$, it shows that the corbel scheme is better than the beam scheme.

Comparative analysis of transverse bending moment of bridge tower under permanent load is shown in Fig. 3. At the bottom of the lower tower column and the bottom of the middle tower column, when $\alpha = 60\%$ and 120%, the corbel scheme is obviously better than the beam scheme. At the top of the middle tower, the bottom of the upper tower and the top of the upper tower, α is close to 0, and the bending moments of the three are basically the same. Only at the top of the lower tower, when $\alpha = -80\%$, he bending moment of the corbel scheme is larger. The bending moment at the bottom of the lower tower column is large, resulting in a large difference in the absolute value of the bending moment at both ends of the lower tower column. The absolute value difference of the bending moment at both ends of the lower tower column is small, and the bending moment distribution is more reasonable in the corbel scheme. Therefore, the corbel scheme is superior to the beam scheme under permanent load, especially at the bottom of the lower tower column and the bottom of the middle tower column. It is suitable to choose the corbel scheme to optimize the design of the bridge tower.

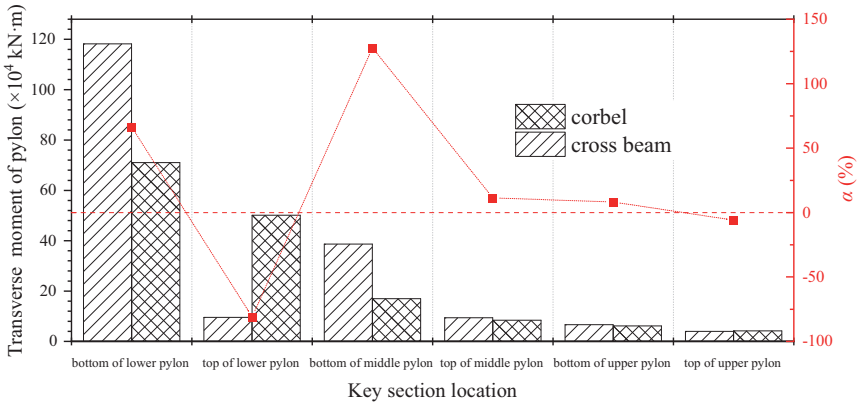

Fig. 3. Comparison of transverse bending moment of the bridge tower under permanent action

3.1.2. The transverse effect of bridge tower under the action of load combination

The transverse bending moment diagram of the bridge tower under the combined action is shown in Fig. 4. The main difference in the bending moment of the bridge tower is reflected in the lower tower column, which is similar to that under permanent load. The transverse bending moment at the bottom of the lower column of the lower beam pylon scheme is 1867643.1 kN·m, while the transverse bending moment at the bottom of the lower column of the open lower corbel pylon scheme is –567749.5 kN·m, and the absolute value difference between the two is 12969893.6 kN·m.

The comparative analysis of transverse bending moment of bridge tower under load combination is shown in Fig. 5. The difference between the bending moment combination values of the two schemes is small at the top and bottom of the upper tower column and the top of the middle tower column, and the α is –3.6%, 5.6% and 4.7%, respectively, indicating that the lateral bending moment of the corbel scheme is similar to that of the beam scheme. At the bottom of the lower tower column, α is 228.9 %, indicating that the corbel scheme can significantly reduce the bending moment at the bottom of the lower tower column.

It is worth noting that the setting of corbel tower will increase the bending moment of the top of the lower tower column and the bottom of the middle tower column, with α of –90.0% and 47.6% respectively. This is due to the fact that the beam is disconnected to reduce the number of statically indeterminate times of the tower structure, and the corbel is a cantilever beam structure, which will increase the bending moment of the top of the lower tower under the action of the support reaction.

In summary, under the combined action of permanent load, vehicle load, temperature load and wind load, the pylon scheme with open lower corbel is obviously better than the scheme with lower beam, especially at the bottom of the lower tower column, it can effectively reduce the transverse bending moment and ensure that the main beam has sufficient longitudinal restraint stiffness.

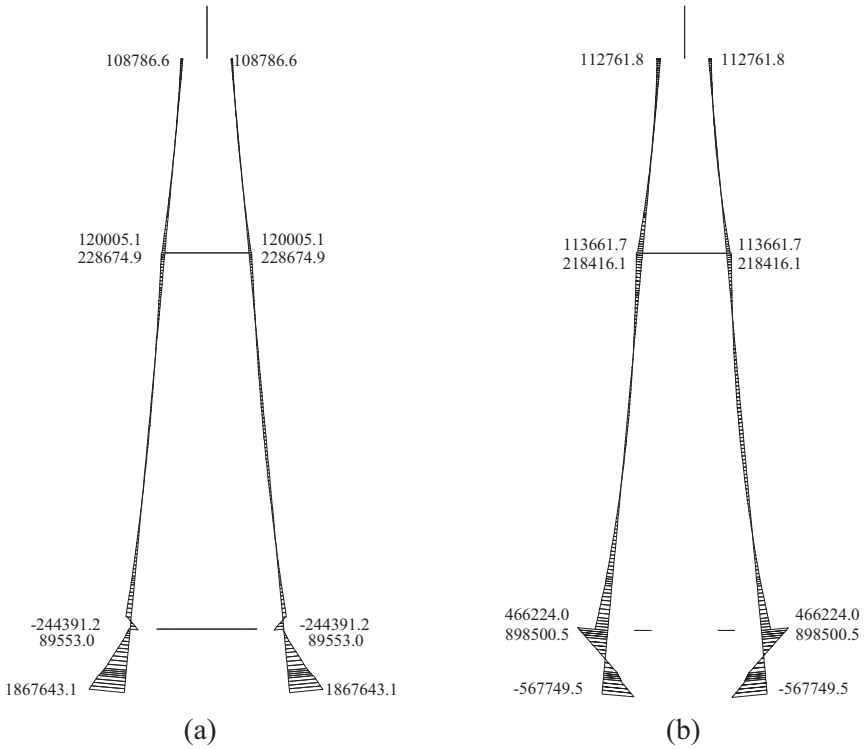

Fig. 4. Transverse bending moment of bridge tower under load combination (kN·m): a) beam scheme, b) corbel scheme

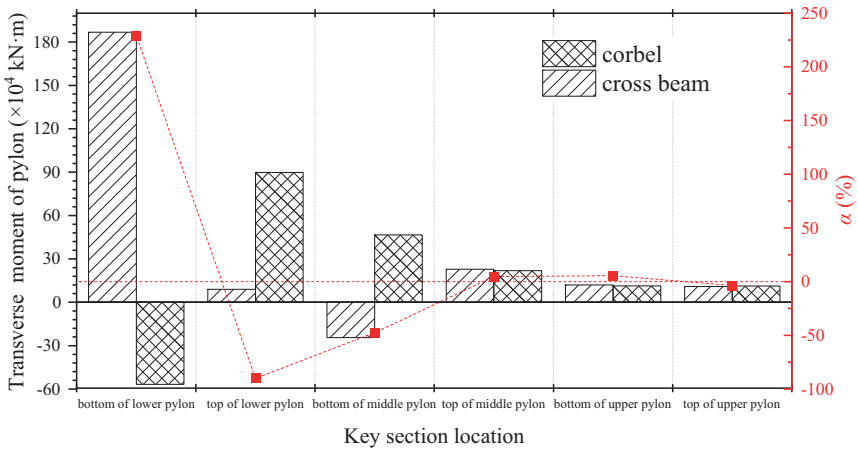

Fig. 5. Comparison of transverse bending moment of bridge tower under load combination

3.2. Lateral stiffness analysis of bridge tower

The displacement diagrams of the bridge tower under the action of vehicle load and wind load are shown in Fig. 6 and Fig. 7.

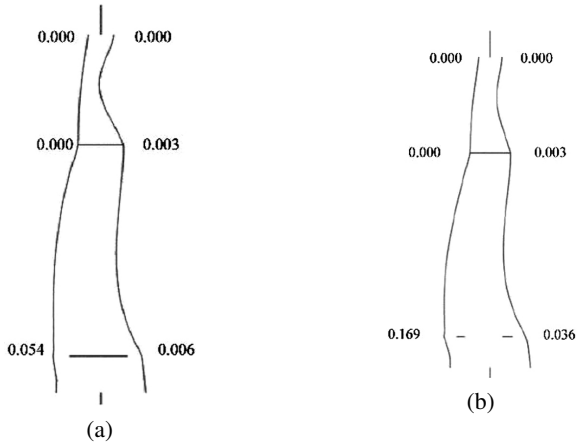

Fig. 6. Transverse deformation of bridge tower under vehicle load (mm):
a) beam scheme, b) corbel scheme

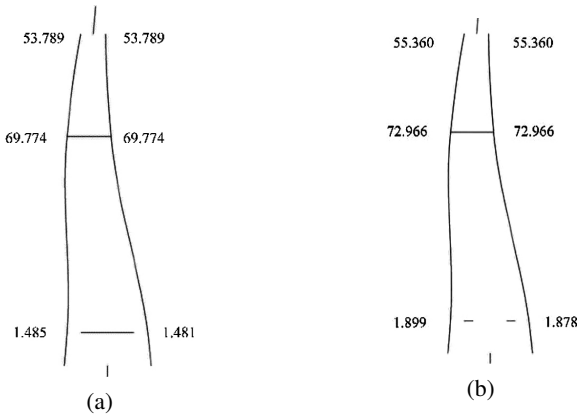

Fig. 7. Transverse deformation of bridge tower under wind load (mm):
a) beam scheme, b) corbel scheme

Under the action of vehicle load, for the beam scheme, there is basically no lateral displacement. For the corbel scheme, the maximum lateral displacement is only 0.2 mm. Wind load is the main lateral load of the bridge tower. The maximum displacement of the bridge tower occurs under the action of wind load on the middle beam, which is 69.7 mm and 73.0 mm respectively. The lower beam is replaced by a corbel, and the overall lateral stiffness of the bridge tower is reduced. However, the decrease in stiffness caused by the corbel can be ignored, due to the large cross-section size of the tower column.

4. Topology optimization of corbels

4.1. Finite element model of corbel

The corbel adopts a single-box double-chamber section, and its specific structural dimensions are shown in Fig. 8. The corbel is 8.769 meters long, with a chamfer of 2 meters × 1 meter at the upper end and a chamfer of 0.5×0.5 meters in the box. The corbel is transversely arranged with prestressed steel strands, and a total of 16 strands of prestressed steel strands are arranged on the top plate. Each strand has 19 strands, with a nominal diameter of $\varphi_s = 15.24$ mm. During the tensioning process, the tension control stress under the anchor is $0.7 f_{pk} = 1302$ MPa, that is, the tension of each strand is 4557 kN.

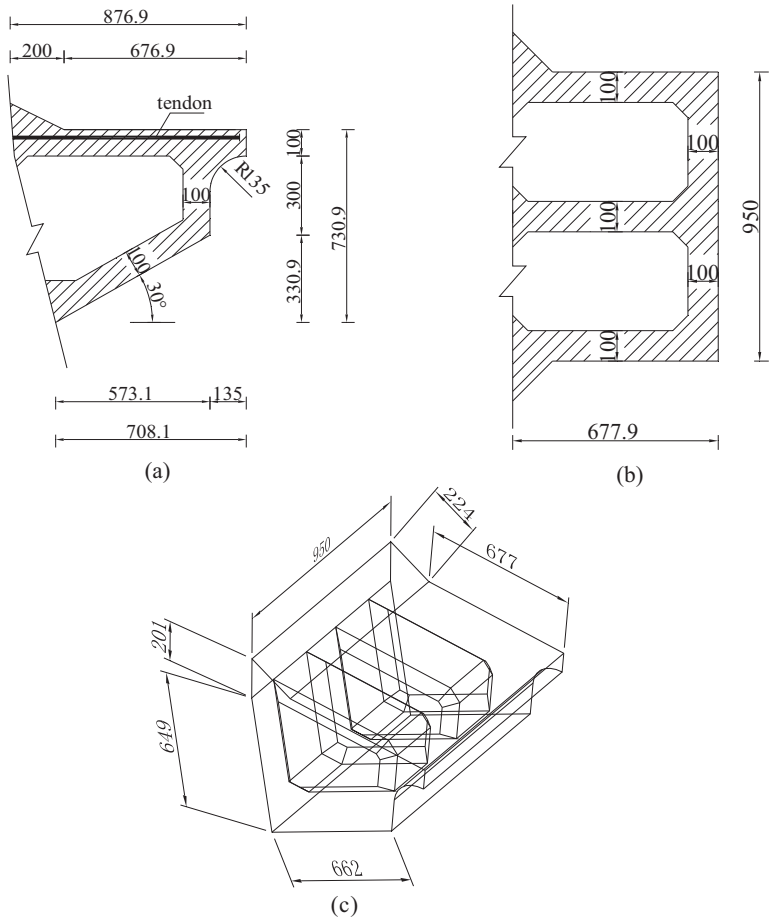

Fig. 8. Schematic diagram of corbel structure (cm): a) vertical profile, b) horizontal section, c) 3D diagram

Only part of the pylon is built in the finite element model, and fixed constraints are applied to the upper and lower top surfaces. The model is shown in Fig. 9. The elastic modulus of concrete is 3.45×104 MPa, density is 26 kN/m^3, Poisson 's ratio is 0.2. The elastic modulus of the steel is 1.95×105 MPa, the density is 78.5 kN/m^3, and the Poisson 's ratio is 0.3 [10]. The tendon is represented in the simulation using bar elements, and the prestressed load, including prestress loss, is simulated through temperature reduction.

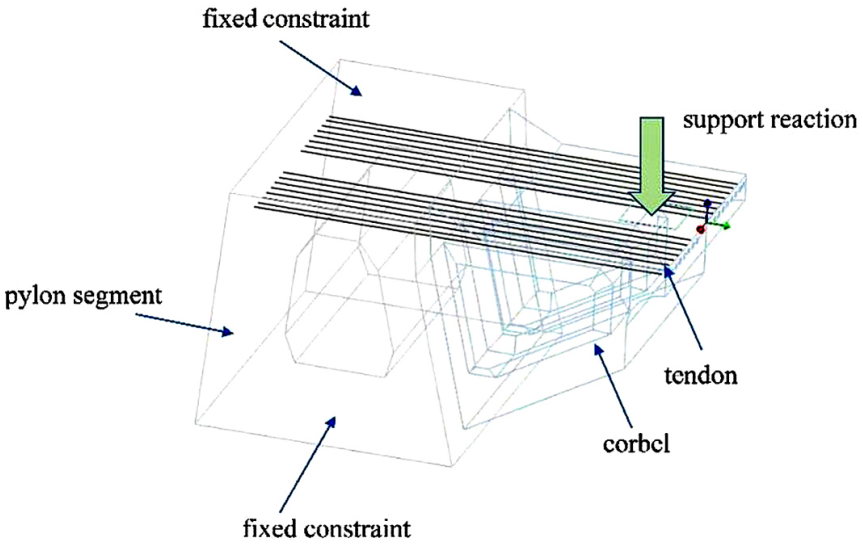

Fig. 9. Analysis model of corbel

4.2. Topological optimization model

Topology optimization is to optimize the structure and save materials while maintaining the load of the structure . [11]. Stress constraints, position constraints and minimum size constraints are required in the topology process of the structure. It can usually be described as [12–15]:

$$\begin{gathered} \text{Find } X = (x_1, x_2, \cdots x_n)^T, \quad 0 \le x_i \le 1 \\ \text{Min } f(x) = f(x^*) \\ \text{s.t. } \sigma_{\max} \le \sigma \\ \delta \le [\delta] \end{gathered} \tag{4.1}$$

where: X is topology optimization variables, x_i is relative density of material, $f(x)$ is objective function, x^* is the most value variable of the optimization results, $\sigma_{\max}$ is maximum stress of element, σ is allowable stress, δ is the upper and lower limits of displacement constraints.

The relative density method is used to create a mathematical model with the minimum strain energy as the objective function [16, 17]:

$$\min_{x} : c(X) = U^T KU = \sum_{e=1}^{N} (x_e)^p u_e^T k_e u_e \tag{4.2}$$

$$\text{subject to: } \frac{V(X)}{V_0} = f$$

$$KU = F$$

$$0 < X_{\min} \leq X \leq 1$$

where: $X = \{x_1, x_2, \cdots, x_N\}$ is design variable. In this paper, it is the strain energy and volume, N is total number of units, F is overall load matrix, U is displacement matrix, K is global stiffness matrix, u_e is element displacement matrix, k_e is element stiffness matrix, f is volumetric coefficient, $V(x)$ is optimized material volume, V_0 is initial material volume, p is penalty factor, generally take as 3 [18, 19].

Considering that the corbel top plate should be arranged with prestressed1 steel strands, all areas except the top plate are selected as the optimization design area.

4.3. Optimal results

The optimized stress results are shown in Fig. 10. The optimized maximum tensile stress is 2.641 MPa and the maximum compressive stress is 5.038 MPa.

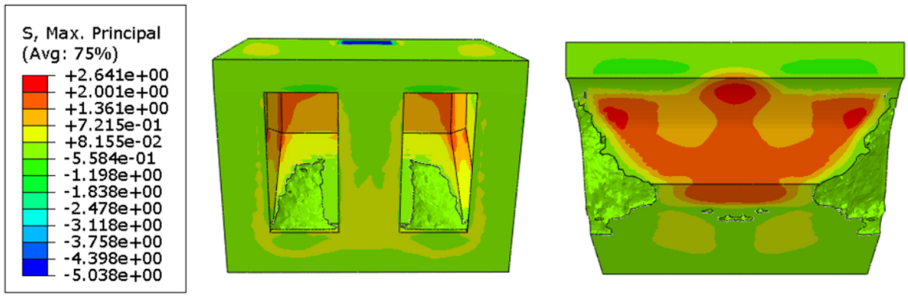

Fig. 10. Optimized stress (MPa)

The interior and exterior of the corbel box floor are reduced as shown in Fig. 10. Only the topology optimization results of the inner box of the corbel are retained, considering the rationality of the actual construction1 of the corbel. The reverse modeling of the optimized model is carried out, considering the actual construction technology and structural shape, the thickness of some sections is adjusted according to the trend of stress distribution. In the reverse modeling, the optimization area is smoothed and some optimization areas are filled. The final corbel optimization model is shown in Fig. 11a. The same size and more regular details excavated in the model double chamber are shown in Fig. 11b, and the thickness of the bottom plate is reduced to 44 cm.

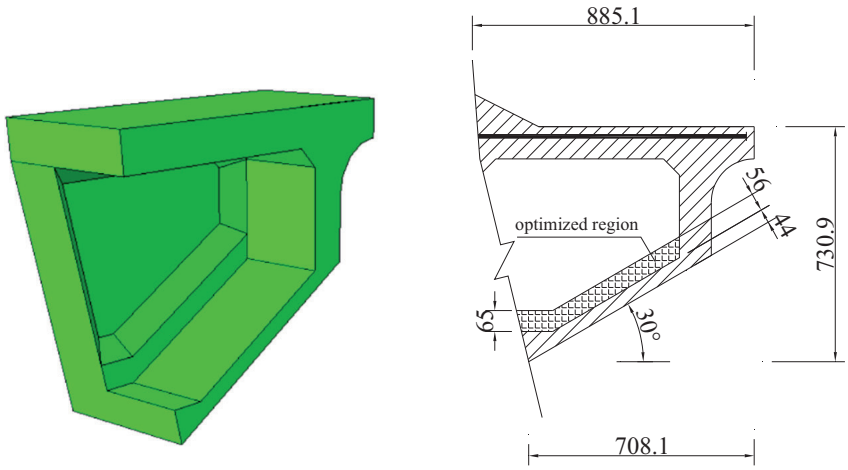

Fig. 11. Final optimization results: a) solid model, b) vertical profile (cm)

The final optimization model is subjected to the same load as the initial model in order to test whether the strength of the final corbel optimization1 scheme meets the requirements. The 1st principal stress cloud diagram and displacement cloud diagram of the optimized model and the original model are compared, and the results are shown in Fig. 12 and Fig. 13.

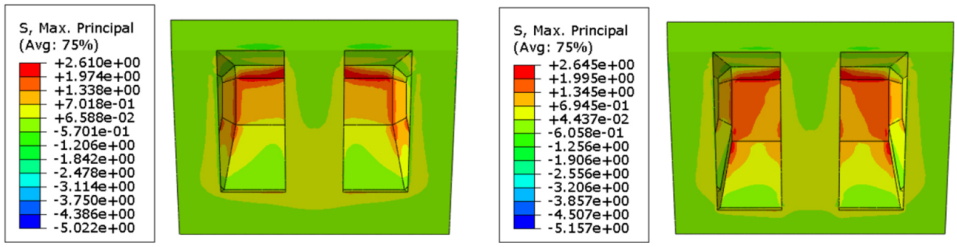

Fig. 12. Comparison of the 1st principal stress (MPa): a) before optimization, b) after optimization

The maximum tensile stress increased by 2.610 MPa to 2.645 MPa after optimization, which met the standard value of tensile strength. At the same time, the maximum deformation after optimization increased from 1.12 mm to 1.22 mm, and the stiffness is basically unchanged. By comparing the volume of the model before and after optimization, the volume of the design area decreased by 8.71% after optimization, and the lightweight design requirements of the corbel were realized.

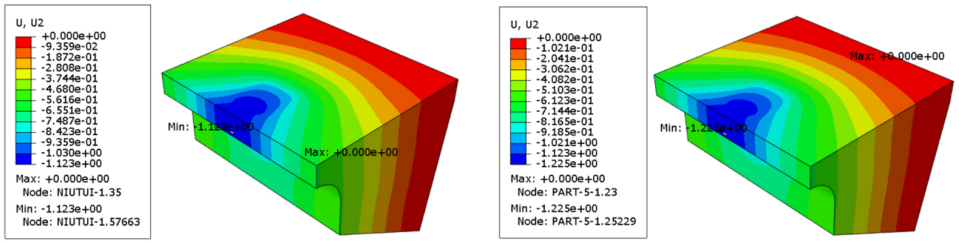

(a) (b)

Fig. 13. Comparison of model displacement (mm): a) before optimization, b) after optimization

5. Conclusions

This study addressed the issue of excessive temperature-induced internal forces in the short lower tower column of the Wuxue Yangtze River Bridge. The proposed open lower corbel tower scheme was analyzed and compared with the traditional lower beam tower scheme. The main findings of the paper are as follows:

1. The adoption of the open lower corbel pylon scheme effectively mitigates the transverse bending moment experienced at the base of the lower tower column. It also ensures that the main beam maintains adequate longitudinal restraint stiffness. The open lower corbel scheme can effectively solve the problem of large temperature secondary internal force caused by shorter lower tower column.
2. While the open lower corbel scheme does reduce the lateral stiffness of the tower, this reduction has a negligible impact due to the tower's substantial cross-sectional dimensions.
3. Topology optimization was performed on the initial corbel design scheme using the relative density method. The optimized design achieved a 56-centimeter reduction in corbel floor thickness and an 8.71% decrease in the volume of the design area. This optimization not only results in material cost savings but also eases the challenge of controlling hydration heat in mass concrete construction.

References

[1] C. Shao, "Composite Girder Cable-Stayed Bridge", in *Cable Supported Composite Bridges*, C. Shao, Ed. Singapore: Springer Nature Singapore, 2023, pp. 65–219, doi: 10.1007/978-981-99-3208-5_3.

[2] W. Podolny and J.F. Fleming, "Historical development of cable-stayed bridges", *Journal of the Structural Division*, vol. 98, no. 9, pp. 2079–2095, 1972.

[3] K. Żółtowski, "Cable-stayed bridges. Basic static schemes", *Archives of Civil Engineering*, vol. 67, no. 4, pp. 5–26, 2021, doi: 10.24425/ace.2021.138483.

[4] D. Su, Y.-S. Liu, X.-T. Li, X.-Y. Chen, and D.-H. Li, "Management path of concrete beam bridge in China from the perspective of sustainable development", *Sustainability*, vol. 12, no. 17, art. no. 7145, 2020, doi: 10.3390/su12177145.

[5] Ö. F. Kültür, A. Al-Masri, and B. Sayin, "Effect of high temperature exposure on design parameters and collapse behavior of reinforced concrete and steel-framed buildings", *Case Studies in Construction Materials*, vol. 17, art. no. e01263, 2022, doi: 10.1016/j.cscm.2022.e01263.

[6] L. Zhu, et al., "Temperature effect on cable force of a special-shaped tied-arch bridge", *Heliyon*, vol. 8, no. 11, art. no. e11253, 2022, doi: 10.1016/j.heliyon.2022.e11253.

[7] M. Ito, "Cable-supported steel bridges: Design problems and solutions", *Journal of Constructional Steel Research,* vol. 39, no. 1, pp. 69–84, 1996, doi: 10.1016/0143-974X(96)00026-0.

[8] C. Song, R. Xiao, B. Sun, Z. Wang, and C. Zhang, "Cable force optimization of cable-stayed bridges: A surrogate model-assisted differential evolution method combined with B-Spline interpolation curves", *Engineering Structures*, vol. 283, art. no. 115856, 2023, doi: 10.1016/j.engstruct.2023.115856.

[9] J. Guo and Z. Guan, "Optimization of the cable forces of completed cable-stayed bridges with differential evolvolution method", *Structures*, vol. 47, pp. 1416-1427, 2023, doi: 10.1016/j.istruc.2022.12.004.

[10] *Specifications for Design of Highway Reinforced Concrete and Prestressed Concrete Bridges and Culverts*, 2018. Available: https://www.nssi.org.cn/nssi/front/108570340.html.

[11] O. Sigmund and K. Maute, "Topology optimization approaches", *Structural and Multidisciplinary Optimization*, vol. 48, no. 6, pp. 1031–1055, 2013, doi: 10.1007/s00158-013-0978-6.

[12] D. Yago, J. Cante, O. Lloberas-Valls, and J. Oliver, "Topology Optimization methods for 3D Structural problems: a comparative study", *Archives of Computational Methods in Engineering*, vol. 29, no. 3, pp. 1525–1567, 2022, doi: 10.1007/s11831-021-09626-2.

[13] H. Han, Y. Guo, S. Chen, and Z. Liu, "Topological constraints in 2D structural topology optimization", *Structural and Multidisciplinary Optimization*, vol. 63, no. 1, pp. 39–58, 2021, doi: 10.1007/s00158-020-02771-5.

[14] G. Fiuk and M. W. Mrzygłód, "Numerical benchmarks for topology optimization of structures with stress constraints", *Bulletin of the Polish Academy of Sciences Technical Sciences*, vol. 69, no. 6, art. no. e139317, 2021, doi: 10.24425/bpasts.2021.139317.

[15] H. Cui, L. Xie, M. Xiao, and M. Deng, "Conceptual design of reinforced concrete structures using truss-like topology optimization", *Archives of Civil Engineering*, vol. 68, no. 3, pp. 523–537, 2022, doi: 10.24425/ace.2022.141900.

[16] S. Shi, P. Zhou, and Z. Lü, "A density-based topology optimization method using radial basis function and its design variable reduction", *Structural and Multidisciplinary Optimization*, vol. 64, no. 4, pp. 2149–2163, 2021, doi: 10.1007/s00158-021-02972-6.

[17] Y. Liu, C. Yang, P. Wei, P. Zhou, and J. Du, "An ODE-driven level-set density method for topology optimization", *Computer Methods in Applied Mechanics and Engineering*, vol. 387, art. no. 114159, 2021, doi: 10.1016/j.cma.2021.114159.

[18] L. Xue, J. Liu, G. Wen, and H. Wang, "Efficient, high-resolution topology optimization method based on convolutional neural networks", *Frontiers of Mechanical Engineering*, vol. 16, no. 1, pp. 80–96, 2021, doi: 10.1007/s11465-020-0614-2.

[19] 1 L. Siva Rama Krishna, N. Mahesh, and N.Sateesh, "Topology optimization using solid isotropic material with penalization technique for additive manufacturing", *Materials Today: Proceedings*, vol. 4, no. 2, Part A, pp. 1414–1422, 2017, doi: 10.1016/j.matpr.2017.01.163.

Received: 2023-11-14, Revised: 2023-12-28